Measurement of the mass and production rate of Ξ_b^- baryons

R. Aaij *et al.*[*]
(LHCb Collaboration)

(Received 21 January 2019; published 22 March 2019)

The first measurement of the production rate of Ξ_b^- baryons in pp collisions relative to that of Λ_b^0 baryons is reported, using data samples collected by the LHCb experiment, and corresponding to integrated luminosities of 1, 2 and 1.6 fb^{-1} at $\sqrt{s} = 7$, 8 and 13 TeV, respectively. In the kinematic region $2 < \eta < 6$ and $p_{\mathrm{T}} < 20$ GeV/c, we measure $\frac{f_{\Xi_b^-}}{f_{\Lambda_b^0}} \frac{\mathcal{B}(\Xi_b^- \to J/\psi \Xi^-)}{\mathcal{B}(\Lambda_b^0 \to J/\psi \Lambda)} = (10.8 \pm 0.9 \pm 0.8) \times 10^{-2}$ [$\sqrt{s} = 7, 8$ TeV], $\frac{f_{\Xi_b^-}}{f_{\Lambda_b^0}} \frac{\mathcal{B}(\Xi_b^- \to J/\psi \Xi^-)}{\mathcal{B}(\Lambda_b^0 \to J/\psi \Lambda)} = (13.1 \pm 1.1 \pm 1.0) \times 10^{-2}$ [$\sqrt{s} = 13$ TeV], where $f_{\Xi_b^-}$ and $f_{\Lambda_b^0}$ are the fragmentation fractions of b quarks into Ξ_b^- and Λ_b^0 baryons, respectively; $\mathcal{B}$ represents branching fractions; and the uncertainties are due to statistical and experimental systematic sources. The values of $f_{\Xi_b^-}/f_{\Lambda_b^0}$ are obtained by invoking SU(3) symmetry in the $\Xi_b^- \to J/\psi \Xi^-$ and $\Lambda_b^0 \to J/\psi \Lambda$ decays. Production asymmetries between Ξ_b^- and $\bar{\Xi}_b^+$ baryons are also reported. The mass of the Ξ_b^- baryon is also measured relative to that of the Λ_b^0 baryon, from which it is found that $m(\Xi_b^-) = 5796.70 \pm 0.39 \pm 0.15 \pm 0.17$ MeV/c^2, where the last uncertainty is due to the precision on the known Λ_b^0 mass. This result represents the most precise determination of the Ξ_b^- mass.

DOI: 10.1103/PhysRevD.99.052006

The decays of beauty (b) quarks provide a sensitive probe of physics within, and beyond, the Standard Model. Due to the large $b\bar{b}$ production cross section at the Large Hadron Collider, beauty hadrons of all species are abundantly produced. Measurements of branching fractions in specific decay channels are often needed in order to make quantitative comparisons to theoretical predictions. However, absolute branching fraction measurements at hadron colliders are difficult to perform without an external input. Instead, one generally resorts to measuring a particular branching fraction relative to that of a topologically similar decay mode, frequently one that involves either a B^0 or a B^- meson, whose absolute branching fractions are known from B-factory measurements. When B_s^0 or Λ_b^0 branching fractions are measured relative to those of a B^0 decay, knowledge of the ratio of fragmentation fractions, f_s/f_d for B_s^0 decays, or $f_{\Lambda_b^0}/f_d$ for Λ_b^0 decays, is required. Here, f_d, f_s and $f_{\Lambda_b^0}$ represent the rates at which a b quark hadronizes into a B^0, B_s^0 or Λ_b^0 hadron, respectively.

Theoretically, the most robust way to measure the b-quark fragmentation fractions is to exploit the well-tested prediction from heavy quark effective theory [1–8] that, to first order, all b hadrons containing a single heavy quark have equal semileptonic decay widths. Such analyses have been carried out by the LHCb experiment at $\sqrt{s} = 7$ TeV [9] and 13 TeV [10], where it was found that $\langle f_s/f_d \rangle \simeq 0.26$ and $\langle f_{\Lambda_b^0}/f_d \rangle \simeq 0.6$, averaged over the pseudorapidity (η) and transverse momentum (p_{T}) region $2 < \eta < 5$ and $3 < p_{\mathrm{T}} < 25$ GeV/c. An alternative technique, which relies on factorization and SU(3) flavor symmetry in the $B_s^0 \to D_s^- \pi^+$ and $B^0 \to D^- K^+$ decays [11], has also been used to measure f_s/f_d, yielding a value consistent with that obtained in semileptonic decays.

With the large samples of b hadrons collected by the LHCb experiment, a number of new decay modes of Ξ_b^0, Ξ_b^-, and even Ω_b^- baryons have been searched for, and in many cases these searches have led to first observations [12–20]. However, when new decay modes of these baryons are observed, absolute branching fractions cannot be determined due to a lack of knowledge of the fragmentation fractions $f_{\Xi_b^0}$, $f_{\Xi_b^-}$ and $f_{\Omega_b^-}$. For example, in one such measurement, evidence of the strangeness-changing weak decay $\Xi_b^- \to \Lambda_b^0 \pi^-$ was reported [16], with the result that $(f_{\Xi_b^-}/f_{\Lambda_b^0}) \mathcal{B}(\Xi_b^- \to \Lambda_b^0 \pi^-) = (5.7 \pm 1.8^{+0.8}_{-0.9}) \times 10^{-4}$. To compute the decay width $\Gamma(\Xi_b^- \to \Lambda_b^0 \pi^-)$ and compare to theoretical predictions requires knowledge of the ratio $f_{\Xi_b^-}/f_{\Lambda_b^0}$.

In principle, the same procedure used to measure f_s/f_d and $f_{\Lambda_b^0}/f_d$ can be applied to semileptonic $\Xi_b^0 \to \Xi_c^+ \mu^- \bar{\nu}_\mu X$

[*]Full author list given at the end of the article.

and $\Xi_b^- \to \Xi_c^0 \mu^- \bar{\nu}_\mu X$ decays to measure $f_{\Xi_b^0}/f_d$ and $f_{\Xi_b^-}/f_d$. However, an obstacle to such an analysis is the limited knowledge of absolute branching fractions for the decays of the Ξ_c^+ or Ξ_c^0 baryon. Recently, the Belle experiment published a first measurement of the absolute branching fractions for three Ξ_c^0 decay modes, each with a relative precision of about 40% [21]. No such measurements exist yet for the Ξ_c^+ baryon. Precise measurements of branching fractions for both Ξ_c^+ and Ξ_c^0 decays should be feasible in the Belle II experiment [22].

Production ratio measurements of the hadronic $\Xi_b^0 \to \Xi_c^+ \pi^-$ and $\Lambda_b^0 \to \Lambda_c^+ \pi^-$ decays [14], where both the Ξ_c^+ and Λ_c^+ baryons are reconstructed in the $pK^-\pi^+$ final state, have been used to predict $f_{\Xi_b^0}/f_{\Lambda_b^0}$. In this case, theoretical estimates of $\mathcal{B}(\Xi_c^+ \to pK^-\pi^+)$ are used, resulting in predictions of $f_{\Xi_b^0}/f_{\Lambda_b^0} = 0.065 \pm 0.020$ [23] and $f_{\Xi_b^0}/f_{\Lambda_b^0} = 0.054 \pm 0.020$ [24].

An alternative approach to either of these two methods is to exploit the decays $\Lambda_b^0 \to J/\psi\Lambda$ and $\Xi_b^- \to J/\psi\Xi^-$, where the Ξ^- baryon is detected in its decay to $\Lambda\pi^-$. Charge-conjugate processes are implicitly included. These decay rates are related through SU(3) flavor symmetry, where one finds [25–27]

$$\frac{\Gamma(\Xi_b^- \to J/\psi\Xi^-)}{\Gamma(\Lambda_b^0 \to J/\psi\Lambda)} = \frac{3}{2}. \tag{1}$$

The ratio

$$R \equiv \frac{f_{\Xi_b^-}}{f_{\Lambda_b^0}} \frac{\mathcal{B}(\Xi_b^- \to J/\psi\Xi^-)}{\mathcal{B}(\Lambda_b^0 \to J/\psi\Lambda)} = \frac{f_{\Xi_b^-}}{f_{\Lambda_b^0}} \frac{\Gamma(\Xi_b^- \to J/\psi\Xi^-)}{\Gamma(\Lambda_b^0 \to J/\psi\Lambda)} \frac{\tau_{\Xi_b^-}}{\tau_{\Lambda_b^0}} \tag{2}$$

depends on $f_{\Xi_b^-}/f_{\Lambda_b^0}$, the partial decay widths Γ, and the lifetimes τ of the indicated b baryons. Experimentally, R is obtained from the ratio of efficiency-corrected yields:

$$R = \frac{N(\Xi_b^- \to J/\psi\Xi^-)}{N(\Lambda_b^0 \to J/\psi\Lambda)} \frac{\epsilon_{\Lambda_b^0}}{\epsilon_{\Xi_b^-}}, \tag{3}$$

where ϵ represents the detection efficiency and N is the yield of the indicated decays.

In this article, we report a first measurement of the ratio R in pp collision data collected by the LHCb experiment, corresponding to integrated luminosities of 1.0 fb^{-1} at $\sqrt{s} = 7$ TeV, 2.0 fb^{-1} at $\sqrt{s} = 8$ TeV and 1.6 fb^{-1} at $\sqrt{s} = 13$ TeV. The measurement of R, along with the SU(3) assumption in Eq. (1) and the known Λ_b^0 and Ξ_b^- baryon lifetimes [28], is used to infer the value of $f_{\Xi_b^-}/f_{\Lambda_b^0}$. The same data samples are also used to measure the production asymmetry between Ξ_b^- and $\bar{\Xi}_b^+$ baryons, and to make the most precise measurement of the Ξ_b^- mass.

The LHCb detector [29,30] is a single-arm forward spectrometer designed for the study of particles containing b or c quarks. The detector includes a high-precision tracking system consisting of a silicon-strip vertex detector surrounding the pp interaction region, a large-area silicon-strip detector located upstream of a dipole magnet with a bending power of about 4 Tm, and three stations of silicon-strip detectors and straw drift tubes placed downstream of the magnet. The tracking system provides a measurement of the momentum, p, of charged particles with a relative uncertainty that varies from 0.5% at low momentum to 1.0% at 200 GeV/c. The minimum distance of a track to a primary vertex (PV), the impact parameter (IP), is measured with a resolution of $(15 + 29/p_{\mathrm{T}})$ μm, where p_{T} is expressed in GeV/c. Different types of charged hadrons are distinguished using information from two ring-imaging Cherenkov detectors. Photons, electrons and hadrons are identified by a calorimeter system consisting of scintillating-pad and preshower detectors, an electromagnetic and a hadronic calorimeter. Muons are identified by a system composed of alternating layers of iron and multiwire proportional chambers. The online event selection is performed by a trigger which consists of a hardware stage, based on information from the calorimeter and muon systems, followed by a software stage, which applies a full event reconstruction.

Simulation is required to model the effects of the detector acceptance and the imposed selection requirements. In the simulation, pp collisions are generated using Pythia [31] with a specific LHCb configuration [32]. Decays of unstable particles are described by EvtGen [33], in which final-state radiation is generated using Photos [34]. The interaction of the generated particles with the detector, and its response, are implemented using the Geant4 toolkit [35] as described in Ref. [36].

The $\Xi_b^- \to J/\psi\Xi^-(\to \Lambda\pi^-)$ and $\Lambda_b^0 \to J/\psi\Lambda$ decays both contain a J/ψ meson and a Λ baryon in the decay chain, and are kinematically similar. To reduce systematic uncertainties, selection requirements are tailored to exploit the common particles in the final state of the Λ_b^0 and Ξ_b^- decays. At the trigger level, both modes are required to satisfy requirements based solely on the $J/\psi \to \mu^+\mu^-$ decay. Firstly, the hardware stage must register either a single high-p_{T} muon or a $\mu^+\mu^-$ pair. The software stage [37] then requires a $\mu^+\mu^-$ pair whose decay vertex is displaced from all PVs in the event, and that has an invariant mass consistent with the known J/ψ mass [28].

Selected events may contain more than one PV. Each particle is associated to the PV for which the corresponding value of χ^2_{IP} is smallest, where χ^2_{IP} is defined as the difference in the vertex-fit χ^2 of a given PV reconstructed with and without the particle under consideration.

In the offline analysis, each muon must have p_{T} in excess of 550 MeV/c and have IP to all PVs in the event that exceeds approximately three times the expected uncertainty. The $\mu^+\mu^-$ pair must form a good-quality vertex and have an invariant mass within 40 MeV/c^2 of the known J/ψ mass, corresponding to about three times the mass resolution.

Reconstructed charged particles are classified into two categories in this analysis. The "long" category refers to tracks that have reconstructed segments in both the vertex detector and the tracking stations upstream and downstream of the LHCb magnet. The "downstream" category consists of those tracks that are not reconstructed in the vertex detector, and thus only include information from the tracking detectors just before and after the LHCb magnet. While most of the reconstructed particles from the pp interactions are in the long category, the decay products of long-lived strange particles tend to be mostly reconstructed as downstream tracks. Because of the presence of vertex detector measurements, the trajectories, and hence the IP, of long tracks are measured with better precision than those of downstream tracks.

Candidate $\Lambda \to p\pi^-$ decays are formed by combining downstream p and π^- candidates with p_{T} in excess of 500 and 100 MeV/c, respectively. Both tracks are required to be significantly detached from all PVs in the event. Together they must form a good-quality vertex and must satisfy the requirement $|M(p\pi^-) - m_\Lambda| < 8$ MeV/c^2, corresponding to approximately three times the mass resolution. Here and throughout the text, M represents an invariant mass and m represents the known mass of the indicated particle [28].

The Ξ^- baryon is reconstructed through its decay to $\Lambda\pi^-$. Due to the long Ξ^- and Λ lifetimes, only Λ candidates formed from downstream tracks are used, as they contribute about 90% to the Ξ^- sample in Ξ_b^- decays. To maintain a uniform selection, the same requirement is imposed on Λ decays in the Λ_b^0 mode. The π^- meson from the Ξ^- decay may be reconstructed as either a long or a downstream track. For the Ξ_b^- mass and production asymmetry measurements, both categories are used. However, for the measurement of R, only the long-track sample is used, since the efficiency for detecting the π^- meson in the decay $\Xi^- \to \Lambda\pi^-$ enters directly in Eq. (3), and long-track efficiencies have been precisely calibrated using a tag-and-probe method [38]. No explicit momentum requirement is applied to the π^- meson, since it typically has low momentum. When necessary, the notation π_{L}^- and π_{D}^- is used to distinguish between long (L) and downstream (D) π^- tracks. Tracks in the π_{L}^- sample are required to be significantly detached from all PVs in the event, corresponding to a requirement that the impact parameter exceeds about four times the corresponding uncertainty; no such requirement is necessary on the π_{D}^- sample. Exploiting the large Ξ^- baryon lifetime, Ξ^- candidates must have $t_{\mathrm{PV}} > 6$ ps, where t_{PV} is the decay time measured relative to the associated PV. Lastly, Ξ^- candidates are required to satisfy the mass requirement $|M(\Lambda\pi_{\mathrm{L,D}}^-) - M(p\pi^-) + m_\Lambda - m_{\Xi^-}| < 10$ MeV/c^2, corresponding to about three times the mass resolution, and have positive decay time, measured relative to the Ξ_b^- decay vertex.

The Λ_b^0 (Ξ_b^-) candidates are formed by combining J/ψ and Λ (Ξ^-) candidates. A vertex fit of good quality is required. To suppress background from prompt J/ψ production, the b hadron is required to have a reconstructed decay time larger than 0.2 ps, which is about four times the resolution. Finally, to have a well-defined fiducial region, the Λ_b^0 and Ξ_b^- candidates are required to be within the kinematic region $2 < \eta < 6$ and $p_{\mathrm{T}} < 20$ GeV/c. Multiple candidates in a single event occur in less than 1% of selected events, and all candidates are kept. To improve the mass resolution, an additional kinematic fit is performed on each candidate, employing both vertex and mass constraints on the J/ψ, Λ and Ξ^- candidates [39]. The resulting mass resolution is about 8 MeV/c^2 for both modes.

The invariant-mass spectra of selected Λ_b^0 and Ξ_b^- candidates are shown in Fig. 1. The data are partitioned into the combined 7, 8 TeV data samples and the 13 TeV data sample, and show the distributions for Λ_b^0 candidates, and Ξ_b^- candidates formed from either long or downstream pions. A simultaneous fit to all six distributions is performed in order to determine the signal yields. Each of the signal shapes is described by the sum of two Crystal Ball (CB) functions [40] with a common peak position and a common width. The tail parameters, which describe the non-Gaussian portion of the signal on either side of the signal peak, are independent for the two CB components. The parameters of the signal shape are determined from large samples of simulated signal decays. The background is described by an exponential function, with the shape parameter left free in the fit to data.

The signal-shape fit parameters are (i) the peak positions, $\bar{m}$, of the Λ_b^0 mass in the 7, 8 TeV and 13 TeV data; (ii) a single mass difference, $\delta m \equiv \bar{m}_{\Xi_b^-} - \bar{m}_{\Lambda_b^0}$; and (iii) a scale factor applied to the simulated width of the CB functions, which allows the mass resolution in data to be slightly different than in simulation. The values of $\bar{m}_{\Lambda_b^0}$ are allowed to differ for the 7, 8 TeV data and the 13 TeV data, since the statistical uncertainty on each is about four times smaller than the systematic uncertainty from the momentum scale calibration [41]. However, that same calibration renders the corresponding uncertainty on δm negligible.

The fitted signal yields and the values of $\bar{m}_{\Lambda_b^0}$ are shown in Table I. From the fit, it is determined that

$$\delta m = 177.30 \pm 0.39 \text{ MeV}/c^2,$$
$$m(\Xi_b^-) = 5796.70 \pm 0.39 \text{ MeV}/c^2,$$

where the uncertainties are statistical only, and we have used $m(\Xi_b^-) = \delta m + m_{\Lambda_b^0}$, with $m_{\Lambda_b^0} = 5619.60 \pm 0.17$ MeV/c^2 [28]. The value of δm is corrected by $+0.12 \pm 0.06$ MeV/c^2 to account for a bias observed in the obtained value of δm, as seen in the fit to large samples of simulated signal decays. The uncertainty on this value is due to the size of the simulated samples.

The ratio of efficiencies in Eq. (3) is determined from weighted simulations of the signal decays. The Λ_b^0

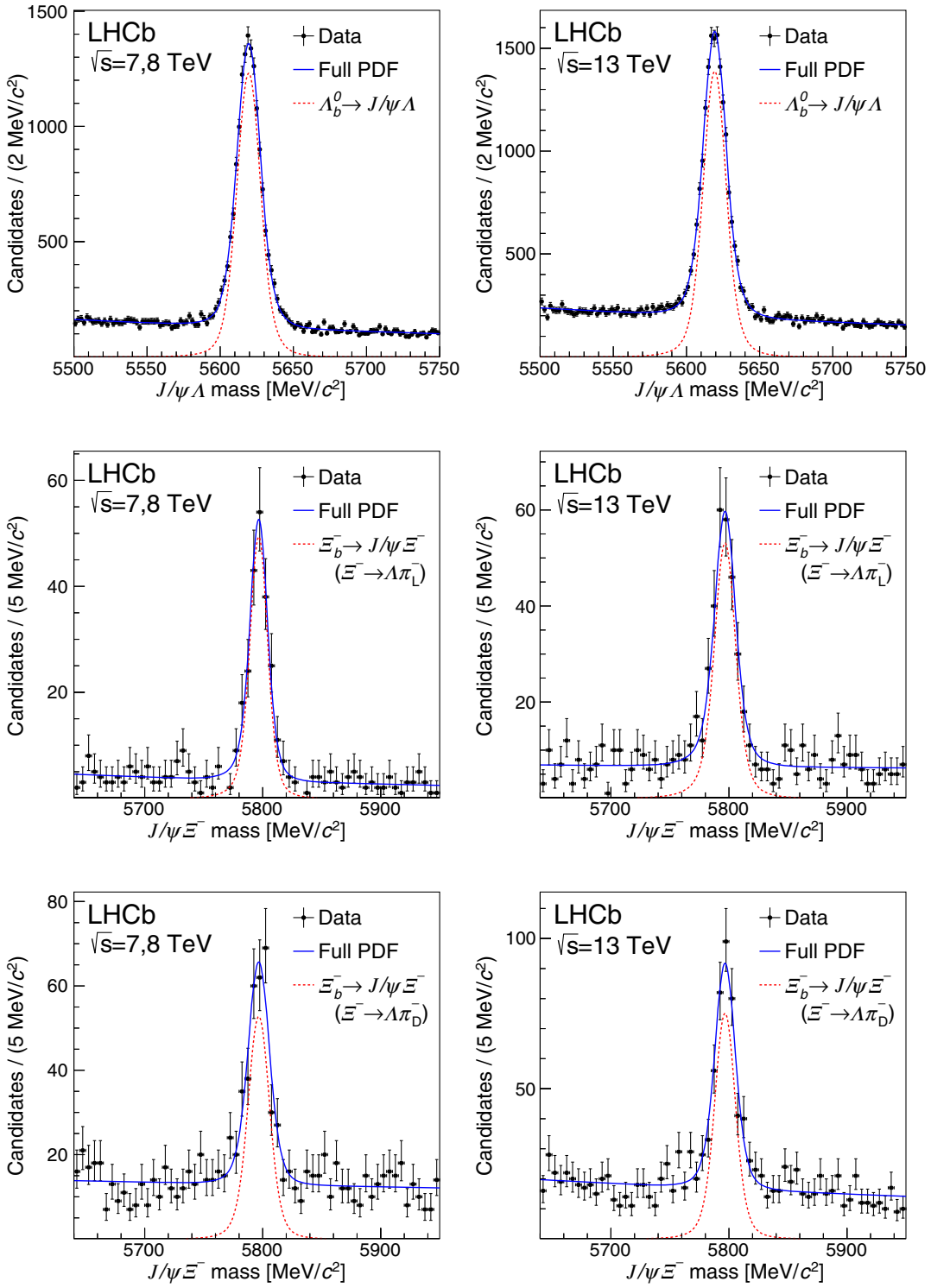

FIG. 1. Invariant-mass distributions for (top) $\Lambda_b^0 \to J/\psi\Lambda$ candidates; (middle) $\Xi_b^- \to J/\psi\Xi^-$, $\Xi^- \to \Lambda\pi_L^-$; and (bottom) $\Xi_b^- \to J/\psi\Xi^-$, $\Xi^- \to \Lambda\pi_D^-$. The subscript on the π^- refers to whether the corresponding track is long or downstream. The left column shows the combined 7 and 8 TeV data and the right one shows the 13 TeV data. The fitted probability distribution functions (PDF) are overlaid.

simulation is weighted in bins of (η, p_T) of the b baryon to reproduce the 2D distribution observed in the data, after the background contribution is subtracted using the *sPlot* method [42]. We assume that the Ξ_b^- spectrum is the same as that of the Λ_b^0, and variations are investigated when assessing systematic uncertainties. By studying the distributions of the fraction of the momentum carried by the decay products in each part of the decay chain, it is found

TABLE I. Fitted signal yields and peak position of the Λ_b^0 signal peak, as obtained from the fit described in the text. The subscript on the π^- refers to whether the corresponding track is long or downstream. The uncertainties shown are statistical only.

	7, 8 TeV	13 TeV
$N(\Lambda_b^0 \to J/\psi\Lambda)$	13307 ± 137	14793 ± 150
$N(\Xi_b^- \to J/\psi\Xi^-, \Xi^- \to \Lambda\pi_{\mathrm{L}}^-)$	203 ± 16	258 ± 22
$N(\Xi_b^- \to J/\psi\Xi^-, \Xi^- \to \Lambda\pi_{\mathrm{D}}^-)$	266 ± 20	357 ± 26
$\bar{m}_{\Lambda_b^0}$ (MeV/c^2)	5619.52 ± 0.09	5619.28 ± 0.09

that the simulation differs from the corresponding spectra observed in data. The simulation is weighted to match the distributions observed in data for the momentum ratio $p_{J/\psi}/p_{\Lambda_b^0}$ and the momentum asymmetry $(p_p - p_{\pi^-})/(p_p + p_{\pi^-})$ in the Λ decay. After this weighting is applied, a large number of other observables are compared, such as decay times, flight distances, p, and p_{T}, and good agreement is found between both Λ_b^0 and Ξ_b^- data and simulation. For the Ξ_b^- sample, only the (η, p_{T}) and $(p_p - p_{\pi^-})/(p_p + p_{\pi^-})$ weights are needed to obtain good agreement with the data.

The resulting efficiencies are summarized in Table II. The efficiencies associated with the detector acceptance, the reconstruction and selection, and the trigger requirements are given, along with the total selection efficiencies. The relative efficiency is approximately 14% for both the 7, 8 TeV and 13 TeV data sets. For the 7, 8 TeV values, the efficiencies represent the weighted average value. This small value is due to the combination of the relatively low momentum and usage of only long tracks for the π^- meson in the Ξ^- decay.

From the signal yields and relative efficiencies, the ratios R are computed to be

$$R = (10.8 \pm 0.9) \times 10^{-2} \quad [\sqrt{s} = 7, 8 \text{ TeV}],$$
$$R = (13.1 \pm 1.1) \times 10^{-2} \quad [\sqrt{s} = 13 \text{ TeV}],$$

where the uncertainties are statistical only.

The difference between the Ξ_b^- and Λ_b^0 baryon production asymmetries is determined using the relation

$$A_{\mathrm{prod}}(\Xi_b^-) - A_{\mathrm{prod}}(\Lambda_b^0) = \alpha(\Xi_b^-) - \alpha(\Lambda_b^0) - A_{\mathrm{det}}(\pi^-), \quad (4)$$

where $\alpha(\Xi_b^-)$ $[\alpha(\Lambda_b^0)]$ is the raw yield asymmetry between the $\Xi_b^- \to J/\psi\Xi^-$ and $\bar{\Xi}_b^+ \to J/\psi\bar{\Xi}^+$ $[\Lambda_b^0 \to J/\psi\Lambda$ and $\bar{\Lambda}_b^0 \to J/\psi\bar{\Lambda}]$ decays. In the difference of the raw yield asymmetries, the Λ detection asymmetry cancels since the kinematical properties are similar. The π^- detection asymmetry, $A_{\mathrm{det}}(\pi^-)$, has been measured [43,44], and, while it is consistent with zero, an asymmetry of up to about 1% in this low momentum region cannot be discounted. In the above expression, it is expected, and assumed, that there is no direct CP violation in these decays.

The raw yield asymmetries are obtained by fitting for the signal yields separately for the beauty baryon and antibaryon subsamples. The fit is similar to that which was described previously, except that the CB width scale factors are fixed to the values obtained from the fit to the full sample, since the mass resolution can be assumed to be the same for the b baryons and antibaryons. The fitted signal yields are shown in Table III, along with the resulting raw asymmetries. The differences in production asymmetries are readily found to be

$$[A_{\mathrm{prod}}(\Xi_b^-) - A_{\mathrm{prod}}(\Lambda_b^0)] = (-1.3 \pm 5.6)\% \quad [\sqrt{s} = 7, 8 \text{ TeV}],$$
$$[A_{\mathrm{prod}}(\Xi_b^-) - A_{\mathrm{prod}}(\Lambda_b^0)] = (-6.3 \pm 4.9)\% \quad [\sqrt{s} = 13 \text{ TeV}],$$

where the uncertainties are due to the signal yields obtained in this analysis.

To obtain $A_{\mathrm{prod}}(\Xi_b^-)$, previous measurements of $A_{\mathrm{prod}}(\Lambda_b^0)$ at $\sqrt{s} = 7$ and 8 TeV are used [45]. Since the value of $A_{\mathrm{prod}}(\Lambda_b^0)$ averaged over the LHCb acceptance is not expected to change significantly with center-of-mass energy [46], and the measured values of $A_{\mathrm{prod}}(\Lambda_b^0)$ obtained at $\sqrt{s} = 7$ and 8 TeV are compatible [45], they are averaged, taking the systematic uncertainties as fully correlated, to obtain $A_{\mathrm{prod}}(\Lambda_b^0) = (2.4 \pm 1.4 \pm 0.9)\%$. An alternate measurement of $A_{\mathrm{prod}}(\Lambda_b^0)$ yielded results that are consistent with the above value [47]. The value at 7, 8 TeV is also used for the Ξ_b^- asymmetry measurement at 13 TeV, and a systematic uncertainty, which is discussed below, is assigned. The Ξ_b^- asymmetries are found to be

TABLE II. Selection efficiencies as obtained from the simulation of $\Lambda_b^0 \to J/\psi\Lambda$ and $\Xi_b^- \to J/\psi\Xi^-$, $\Xi^- \to \Lambda\pi_{\mathrm{L}}^-$ decays at $\sqrt{s} = 7$, 8 TeV and 13 TeV. The efficiencies (ϵ) listed are those associated with the detector acceptance (acc), the reconstruction and selection (sel), the trigger (trig), their product, and the relative efficiency.

	7, 8 TeV		13 TeV	
Final state	$\Lambda_b^0 \to J/\psi\Lambda$	$\Xi_b^- \to J/\psi\Xi^-$	$\Lambda_b^0 \to J/\psi\Lambda$	$\Xi_b^- \to J/\psi\Xi^-$
ϵ_{acc} (%)	18.9 ± 0.1	17.3 ± 0.1	19.8 ± 0.1	18.0 ± 0.1
ϵ_{sel} (%)	2.86 ± 0.02	0.42 ± 0.01	2.91 ± 0.01	0.42 ± 0.01
ϵ_{trig} (%)	73.2 ± 0.3	75.6 ± 0.7	75.4 ± 0.2	77.8 ± 0.5
ϵ (10^{-2}%)	39.5 ± 0.4	5.56 ± 0.11	43.5 ± 0.3	5.85 ± 0.06
$\epsilon_{\Xi_b^-}/\epsilon_{\Lambda_b^0}$ (%)	14.1 ± 0.3		13.4 ± 0.2	

TABLE III. Yields of Λ_b^0 and Ξ_b^- decays, split by the charge of the final state, and their asymmetries, for the combined 7, 8 TeV data samples and the 13 TeV data sample. Uncertainties are statistical only.

	$\Lambda_b^0 \to J/\psi\Lambda$		$\Xi_b^- \to J/\psi\Xi^-$	
	Λ_b^0	$\bar{\Lambda}_b^0$	Ξ_b^-	$\bar{\Xi}_b^+$
$N_{\sqrt{s}=7,8\ \mathrm{TeV}}$	6827 ± 94	6480 ± 92	236 ± 18	230 ± 18
$\alpha_{\sqrt{s}=7,8\ \mathrm{TeV}}$	$(2.6 \pm 1.0)\%$		$(1.3 \pm 5.4)\%$	
$N_{\sqrt{s}=13\ \mathrm{TeV}}$	7602 ± 102	7182 ± 99	304 ± 21	326 ± 22
$\alpha_{\sqrt{s}=13\ \mathrm{TeV}}$	$(2.8 \pm 1.0)\%$		$(-3.5 \pm 4.8)\%$	

$$A_{\mathrm{prod}}(\Xi_b^-) = (1.1 \pm 5.6)\% \quad [\sqrt{s} = 7, 8\ \mathrm{TeV}],$$
$$A_{\mathrm{prod}}(\Xi_b^-) = (-3.9 \pm 4.9)\% \quad [\sqrt{s} = 13\ \mathrm{TeV}].$$

In the mass measurement, most sources of systematic uncertainty cancel, since it relies on the mass difference, δm. The modulus of the correction of $0.12\ \mathrm{MeV}/c^2$ described previously is assigned as a systematic uncertainty. The signal shape uncertainty is quantified by performing an alternate fit using the sum of two Gaussian functions. Apart from a common peak value, all shape parameters are left free in the fit. The difference with respect to the nominal value, $0.06\ \mathrm{MeV}/c^2$, is assigned as a systematic uncertainty. The background shape uncertainty is assessed by using a first-order polynomial in place of the nominal exponential function, and is found to change the result by $0.01\ \mathrm{MeV}/c^2$. The systematic uncertainties due to the momentum scale and energy loss have been evaluated previously [48] and are found to contribute $0.01\ \mathrm{MeV}/c^2$ each. Knowledge of the Ξ^- mass contributes an uncertainty of $0.07\ \mathrm{MeV}/c^2$. Adding these uncertainties in quadrature, the total systematic uncertainty on δm is $0.15\ \mathrm{MeV}/c^2$.

For the measurement of R, several sources of uncertainty are considered, which are summarized in Table IV. The efficiency for all decay products to be within the LHCb acceptance is derived from the simulation, and could depend on the polarization of the Λ_b^0 or Ξ_b^- baryon. To investigate this effect, variations in the Λ_b^0 and Ξ_b^- polarization are considered, including full polarization, zero polarization, and using the helicity amplitudes presented in Ref. [49]. All three variations are found to give statistically compatible acceptance corrections. The assigned uncertainty of 3.0% reflects the statistical precision of the test.

TABLE IV. Summary of relative systematic uncertainties on the production ratio R.

Source	Value (%)
Λ_b^0, Ξ_b^- polarization	3.0
Signal and background shape	2.0
Ξ_b^- production spectra	3.0
π^- tracking efficiency	4.5
Ξ^- mass resolution and nonresonant $\Lambda\pi^-$	3.0
Ξ^- selections	1.4
Ξ_b^- lifetime	0.5
Simulated sample sizes	2.0
Total	7.6

The systematic uncertainty due to the signal and background functions is estimated by using alternate choices for each, as described above for the uncertainty on δm, leading to an uncertainty of 2.0%. The Λ_b^0 and Ξ_b^- simulations are weighted as discussed previously and reproduce well the kinematical distributions of the final-state particles seen in data. However, due to low Ξ_b^- signal yields, variations with respect to the nominal weighting are considered. In particular, a 3% change in the relative efficiency is seen when applying an additional weight to the Ξ_b^- pseudorapidity spectrum that is permissible by the data. A significantly smaller difference is seen when weighting the Ξ_b^- baryon's p_{T} spectrum. A 3% uncertainty is therefore assigned to account for potential differences in the (η, p_{T}) spectrum of Λ_b^0 and Ξ_b^- baryons.

Uncertainties in the detection efficiency of the π^- meson from the Ξ^- decay enters directly into the result for the ratio R. The tracking efficiency in simulation has been calibrated using a tag-and-probe method [38] using $J/\psi \to \mu^+\mu^-$ decays; however, the calibration only covers the kinematic region $p > 5\ \mathrm{GeV}/c$ and $1.9 < \eta < 4.9$. Outside this region, no correction to the tracking efficiency in simulation is applied and an uncertainty of 5% is assigned to the tracking efficiency. This value is justified based upon a comparison of the reconstructed momentum spectrum of π^- mesons from $\Lambda_b^0 \to J/\psi\Lambda$ decays in data and simulation, where the Λ baryons are formed from long tracks. These tracks serve as a good proxy for the π^- meson from Ξ^- baryon decay, since they also have low momentum and large impact parameter. Averaging over the tracks within and outside the range covered by the tracking calibration, an uncertainty of 4.5% on the π^- tracking efficiency is obtained. As a cross-check, the analysis is repeated using only π^- candidates in the range covered by the calibration, and the R values are consistent with the nominal results.

Potential uncertainties due to the Ξ^- mass requirement may arise from differences in the Ξ^- mass resolution, or possibly a (Cabibbo-suppressed) nonresonant $\Lambda\pi^-$

contribution. To quantify the potential size of such effects, the Ξ_b^- signal yield in the Ξ^- sideband region, $10 < |M(\Lambda\pi^-_{\mathrm{L,D}}) - M(p\pi^-) + m_\Lambda - m_{\Xi^-}| < 20\ \mathrm{MeV}/c^2$ is measured. The yield in that region, which is consistent with zero, is taken as a systematic uncertainty. Other Ξ^- selections are very loose and are studied by comparing background-subtracted distributions of relevant variables in data with those in simulation. From the observed differences an uncertainty of 1.4% is assigned. The uncertainty on R due to the knowledge of the Ξ_b^- lifetime, $\tau_{\Xi_b^-} = 1.571 \pm 0.040$ ps [28], is estimated by weighting the simulation to replicate 0.04 ps shorter and longer lifetimes. The effect on R of the Λ_b^0 lifetime uncertainty is negligible. Lastly, the simulated sample sizes contribute 2.0% uncertainty to the relative efficiency.

The uncertainty on the Ξ_b^- production asymmetry receives contributions from the π^- detection asymmetry and the measurement of $A_{\mathrm{prod}}(\Lambda_b^0)$. The pion detection asymmetry uncertainty is assigned to be 1%, as mentioned previously. Taking the sum in quadrature of the statistical and systematic uncertainties in the value of $A_{\mathrm{prod}}(\Lambda_b^0) = (2.4 \pm 1.4 \pm 0.9)\%$, a 1.7% systematic uncertainty is assigned. Since the average value of $A_{\mathrm{prod}}(\Lambda_b^0)$ at $\sqrt{s} = 7$ and 8 TeV [45] could differ from that at 13 TeV [46], an additional systematic uncertainty of 1.5% is assigned to the measured value of $A_{\mathrm{prod}}(\Xi_b^-)$ at 13 TeV. The total systematic uncertainty in $A_{\mathrm{prod}}(\Xi_b^-)$ is therefore 1.9% and 2.5% for the 7, 8 TeV and 13 TeV data samples, respectively.

In summary, data samples collected at $\sqrt{s} = 7$, 8 and 13 TeV have been used to measure the ratio of production rates of Ξ_b^- and Λ_b^0 baryons in the pseudorapidity and p_{T} region, $2 < \eta < 6$ and $p_{\mathrm{T}} < 20\ \mathrm{GeV}/c$, to be

$$R = (10.8 \pm 0.9 \pm 0.8) \times 10^{-2} \quad [\sqrt{s} = 7, 8\ \mathrm{TeV}],$$
$$R = (13.1 \pm 1.1 \pm 1.0) \times 10^{-2} \quad [\sqrt{s} = 13\ \mathrm{TeV}],$$

where the uncertainties are statistical and systematic. From the values of R, the ratios of fragmentation fractions are determined to be

$$\frac{f_{\Xi_b^-}}{f_{\Lambda_b^0}} = (6.7 \pm 0.5 \pm 0.5 \pm 2.0) \times 10^{-2} \quad [\sqrt{s} = 7, 8\ \mathrm{TeV}],$$
$$\frac{f_{\Xi_b^-}}{f_{\Lambda_b^0}} = (8.2 \pm 0.7 \pm 0.6 \pm 2.5) \times 10^{-2} \quad [\sqrt{s} = 13\ \mathrm{TeV}].$$

The last uncertainty, due to the assumed SU(3) flavor symmetry and taken to be 30%, is an estimate of the typical size of SU(3)-breaking effects between decays related by this symmetry. The LHCb results show no significant dependence on the center-of-mass energy in the 7 to 13 TeV range. These results are consistent with the predictions in Refs. [23,24], which used production ratio measurements of $\Xi_b^0 \to \Xi_c^+\pi^-$ and $\Lambda_b^0 \to \Lambda_c^+\pi^-$ decays at 7 and 8 TeV [14] and an estimated value for $\mathcal{B}(\Xi_c^+ \to pK^-\pi^+)$. Assuming that $f_{\Xi_b^0} \approx f_{\Xi_b^-}$, these results indicate that in the forward region, b quarks fragment into Ξ_b baryons at about 15% of the rate at which they fragment into Λ_b^0 baryons. Previous measurements of R by the CDF [50] and D0 [51] collaborations are about two standard deviations larger than the results reported here; however, those measurements are performed in $p\bar{p}$ collisions at $\sqrt{s} = 2$ TeV and in the central rapidity region $|\eta| < 2$.

The mass difference, δm, and the corresponding value of the Ξ_b^- mass, $m(\Xi_b^-)$, are measured to be

$$\delta m = 177.30 \pm 0.39 \pm 0.15\ \mathrm{MeV}/c^2,$$
$$m(\Xi_b^-) = 5796.70 \pm 0.39 \pm 0.15 \pm 0.17\ \mathrm{MeV}/c^2,$$

where the last uncertainty is due to the Λ_b^0 mass. This Ξ_b^- mass measurement includes the data used in Ref. [48], and therefore supersedes those results. This measurement represents the most precise determination of the Ξ_b^- mass, and is consistent with the previous most precise measurement of the mass difference of $178.36 \pm 0.46 \pm 0.16\ \mathrm{MeV}/c^2$ [15].

The Ξ_b^- production asymmetry is also measured for the first time. The values at the lower and higher center-of-mass energies are

$$A_{\mathrm{prod}}(\Xi_b^-) = (1.1 \pm 5.6 \pm 1.9)\% \quad [\sqrt{s} = 7, 8\ \mathrm{TeV}],$$
$$A_{\mathrm{prod}}(\Xi_b^-) = (-3.9 \pm 4.9 \pm 2.5)\% \quad [\sqrt{s} = 13\ \mathrm{TeV}].$$

The asymmetries are consistent with zero at the level of a few percent.

We thank M. Voloshin for interesting and helpful discussions on theoretical aspects of this work. We express our gratitude to our colleagues in the CERN accelerator departments for the excellent performance of the LHC. We thank the technical and administrative staff at the LHCb institutes. We acknowledge support from CERN and from the national agencies: CAPES, CNPq, FAPERJ and FINEP (Brazil); MOST and NSFC (China); CNRS/IN2P3 (France); BMBF, DFG and MPG (Germany); INFN (Italy); NWO (Netherlands); MNiSW and NCN (Poland); MEN/IFA (Romania); MSHE (Russia); MinECo (Spain); SNSF and SER (Switzerland); NASU (Ukraine); STFC (United Kingdom); and NSF (USA). We acknowledge the computing resources that are provided by CERN, IN2P3 (France), KIT and DESY (Germany), INFN (Italy), SURF (Netherlands), PIC (Spain), GridPP (United Kingdom), RRCKI and Yandex LLC (Russia), CSCS (Switzerland), IFIN-HH (Romania), CBPF (Brazil), PL-GRID (Poland) and OSC (USA). We are indebted to the communities behind the multiple open-source software packages on which we depend. Individual groups or

members have received support from AvH Foundation (Germany); EPLANET, Marie Skłodowska-Curie Actions and ERC (European Union); ANR, Labex P2IO and OCEVU, and Région Auvergne-Rhône-Alpes (France); Key Research Program of Frontier Sciences of CAS, CAS PIFI, and the Thousand Talents Program (China); RFBR, RSF and Yandex LLC (Russia); GVA, XuntaGal and GENCAT (Spain); the Royal Society and the Leverhulme Trust (United Kingdom); Laboratory Directed Research and Development program of LANL (USA).

[1] V. A. Khoze and M. A. Shifman, Heavy quarks, Sov. Phys. Usp. **26**, 387 (1983).
[2] I. I. Bigi and N. G. Uraltsev, Gluonic enhancements in non-spectator beauty decays—An inclusive mirage though an exclusive possibility, Phys. Lett. B **280**, 271 (1992).
[3] I. I. Bigi, N. G. Uraltsev, and A. I. Vainshtein, Nonperturbative corrections to inclusive beauty and charm decays. QCD versus phenomenological models, Phys. Lett. B **293**, 430 (1992); Erratum, Phys. Lett. B **297**, 477(E) (1992).
[4] B. Blok and M. Shifman, The rule of discarding $1/N_c$ in inclusive weak decays (I), Nucl. Phys. **B399**, 441 (1993).
[5] B. Blok and M. Shifman, The rule of discarding $1/N_c$ in inclusive weak decays (II), Nucl. Phys. **B399**, 459 (1993).
[6] M. Neubert, *B* decays and the heavy quark expansion, Adv. Ser. Dir. High Energy Phys. **15**, 239 (1998).
[7] N. Uraltsev, Heavy quark expansion in beauty and its decays, Proceedings of the International School of Physics "Enrico Fermi" **137**, 329 (1998), arXiv:hep-ph/9804275.
[8] G. Bellini, I. I. Y. Bigi, and P. J. Dornan, Lifetimes of charm and beauty hadrons, Phys. Rep. **289**, 1 (1997).
[9] R. Aaij *et al.* (LHCb Collaboration), Measurement of *b* hadron production fractions in 7 TeV pp collisions, Phys. Rev. D **85**, 032008 (2012).
[10] R. Aaij *et al.* (LHCb Collaboration), Measurement of *b*-hadron fractions in 13 TeV pp collisions, arXiv:1902.06794.
[11] R. Aaij *et al.* (LHCb Collaboration), Measurement of the fragmentation fraction ratio f_s/f_d and its dependence on *B* meson kinematics, J. High Energy Phys. 04 (2013) 001.
[12] R. Aaij *et al.* (LHCb Collaboration), Study of beauty baryon decays to D^0ph^- and $\Lambda_c^+h^-$ final states, Phys. Rev. D **89**, 032001 (2014).
[13] R. Aaij *et al.* (LHCb Collaboration), Searches for Λ_b^0 and Ξ_b^0 decays to $K_S^0p\pi^-$ and $K_S^0pK^-$ final states with first observation of the $\Lambda_b^0 \to K_S^0p\pi^-$ decay, J. High Energy Phys. 04 (2014) 087.
[14] R. Aaij *et al.* (LHCb Collaboration), Precision Measurement of the Mass and Lifetime of the Ξ_b^0 Baryon, Phys. Rev. Lett. **113**, 032001 (2014).
[15] R. Aaij *et al.* (LHCb Collaboration), Precision Measurement of the Mass and Lifetime of the Ξ_b^- Baryon, Phys. Rev. Lett. **113**, 242002 (2014).
[16] R. Aaij *et al.* (LHCb Collaboration), Evidence for the Strangeness-Changing Weak Decay $\Xi_b^- \to \Lambda_b^0\pi^-$, Phys. Rev. Lett. **115**, 241801 (2015).
[17] R. Aaij *et al.* (LHCb Collaboration), Observations of $\Lambda_b^0 \to \Lambda K^+\pi^-$ and $\Lambda_b^0 \to \Lambda K^+K^-$ decays and searches for other Λ_b^0 and Ξ_b^0 decays to Λh^+h^- final states, J. High Energy Phys. 05 (2016) 081.
[18] R. Aaij *et al.* (LHCb Collaboration), Observation of the Decay $\Xi_b^- \to pK^-K^-$, Phys. Rev. Lett. **118**, 071801 (2017).
[19] R. Aaij *et al.* (LHCb Collaboration), Observation of the $\Xi_b^- \to J/\psi\Lambda K^-$ decay, Phys. Lett. B **772**, 265 (2017).
[20] R. Aaij *et al.* (LHCb Collaboration), Measurement of branching fractions of charmless four-body Λ_b^0 and Ξ_b^0 decays, J. High Energy Phys. 02 (2018) 098.
[21] Y. B. Li *et al.* (Belle Collaboration), First measurements of absolute branching fractions of Ξ_c^0 at Belle, Phys. Rev. Lett. **122**, 082001 (2019).
[22] T. Abe *et al.* (Belle II Collaboration), Belle II technical design report, arXiv:1011.0352.
[23] D. Wang, Sum rules for *CP* asymmetries of charmed baryon decays in the flavor SU(3) limit, arXiv:1901.01776.
[24] H.-Y. Jiang and F.-S. Yu, Fragmentation-fraction ratio $f_{\Xi_b}/f_{\Lambda_b^0}$ in *b*- and *c*-baryon decays, Eur. Phys. J. C **78**, 224 (2018).
[25] M. J. Savage and M. B. Wise, SU(3) predictions for non-leptonic *B* meson decays to charmed baryons, Nucl. Phys. **B326**, 15 (1989).
[26] M. Voloshin, Remarks on measurement of the decay $\Xi_b^- \to \Lambda_b^0\pi^-$, arXiv:1510.05568.
[27] Y. K. Hsiao, P. Y. Lin, L. W. Luo, and C. Q. Geng, Fragmentation fractions of two-body *b*-baryon decays, Phys. Lett. B **751**, 127 (2015).
[28] M. Tanabashi *et al.* (Particle Data Group), Review of particle physics, Phys. Rev. D **98**, 030001 (2018).
[29] A. A. Alves, Jr. *et al.* (LHCb Collaboration), The LHCb detector at the LHC, J. Instrum. **3**, S08005 (2008).
[30] R. Aaij *et al.* (LHCb Collaboration), LHCb detector performance, Int. J. Mod. Phys. A **30**, 1530022 (2015).
[31] T. Sjöstrand, S. Mrenna, and P. Skands, PYTHIA 6.4 physics and manual, J. High Energy Phys. 05 (2006) 026; A brief introduction to PYTHIA 8.1, Comput. Phys. Commun. **178**, 852 (2008).
[32] I. Belyaev *et al.*, Handling of the generation of primary events in Gauss, the LHCb simulation framework, J. Phys. Conf. Ser. **331**, 032047 (2011).
[33] D. J. Lange, The EvtGen particle decay simulation package, Nucl. Instrum. Methods Phys. Res., Sect. A **462**, 152 (2001).
[34] P. Golonka and Z. Was, PHOTOS Monte Carlo: A precision tool for QED corrections in *Z* and *W* decays, Eur. Phys. J. C **45**, 97 (2006).
[35] J. Allison *et al.* (Geant4 Collaboration), Geant4 developments and applications, IEEE Trans. Nucl. Sci. **53**, 270 (2006); S. Agostinelli *et al.* (Geant4 Collaboration), Geant4:

A simulation toolkit, Nucl. Instrum. Methods Phys. Res., Sect. A **506**, 250 (2003).
[36] M. Clemencic, G. Corti, S. Easo, C. R. Jones, S. Miglioranzi, M. Pappagallo, and P. Robbe, The LHCb simulation application, Gauss: Design, evolution and experience, J. Phys. Conf. Ser. **331**, 032023 (2011).
[37] R. Aaij *et al.*, The LHCb trigger and its performance in 2011, J. Instrum. **8**, P04022 (2013).
[38] R. Aaij *et al.* (LHCb Collaboration), Measurement of the track reconstruction efficiency at LHCb, J. Instrum. **10**, P02007 (2015).
[39] W. D. Hulsbergen, Decay chain fitting with a Kalman filter, Nucl. Instrum. Methods Phys. Res., Sect. A **552**, 566 (2005).
[40] T. Skwarnicki, A study of the radiative cascade transitions between the Upsilon-prime and Upsilon resonances, Ph.D. thesis, Institute of Nuclear Physics, Krakow, 1986.
[41] R. Aaij *et al.* (LHCb Collaboration), Precision measurement of D meson mass differences, J. High Energy Phys. 06 (2013) 065.
[42] M. Pivk and F. R. Le Diberder, sPlot: A statistical tool to unfold data distributions, Nucl. Instrum. Methods Phys. Res., Sect. A **555**, 356 (2005).
[43] R. Aaij *et al.* (LHCb Collaboration), Measurement of the CP Asymmetry in B_s^0–$\bar{B}_s^0$ Mixing, Phys. Rev. Lett. **117**, 061803 (2016).
[44] R. Aaij *et al.* (LHCb Collaboration), Measurement of $D_s^{\pm}$ production asymmetry in pp collisions at $\sqrt{s} = 7$ and 8 TeV, J. High Energy Phys. 08 (2018) 008.
[45] R. Aaij *et al.* (LHCb Collaboration), Measurement of B^0, B_s^0, B^+ and Λ_b^0 production asymmetries in 7 and 8 TeV pp collisions, Phys. Lett. B **774**, 139 (2017).
[46] W. K. Lai and A. K. Leibovich, $\Lambda_c^+/\bar{\Lambda}_c^-$ and $\Lambda_b^0/\bar{\Lambda}_b^0$ production asymmetry at the LHC from heavy quark recombination, Phys. Rev. D **91**, 054022 (2015).
[47] R. Aaij *et al.* (LHCb Collaboration), Study of the productions of Λ_b^0 and $\bar{B}^0$ hadrons in pp collisions and first measurement of the $\Lambda_b^0 \to J/\psi p K^-$ branching fraction, Chin. Phys. C **40**, 011001 (2016).
[48] R. Aaij *et al.* (LHCb Collaboration), Measurements of the Λ_b^0, Ξ_b^-, and Ω_b^- Baryon Masses, Phys. Rev. Lett. **110**, 182001 (2013).
[49] R. Aaij *et al.* (LHCb Collaboration), Measurements of the $\Lambda_b^0 \to J/\psi\Lambda$ decay amplitudes and the Λ_b^0 polarisation in pp collisions at $\sqrt{s} = 7$ TeV, Phys. Lett. B **724**, 27 (2013).
[50] T. Aaltonen *et al.* (CDF Collaboration), Observation of the Ω_b^- and measurement of the properties of the Ξ_b^- and Ω_b^- baryons, Phys. Rev. D **80**, 072003 (2009).
[51] V. M. Abazov *et al.* (D0 Collaboration), Direct Observation of the Strange b Baryon Ξ_b^-, Phys. Rev. Lett. **99**, 052001 (2007).

R. Aaij,[28] C. Abellán Beteta,[46] B. Adeva,[43] M. Adinolfi,[50] C. A. Aidala,[77] Z. Ajaltouni,[6] S. Akar,[61] P. Albicocco,[19] J. Albrecht,[11] F. Alessio,[44] M. Alexander,[55] A. Alfonso Albero,[42] G. Alkhazov,[41] P. Alvarez Cartelle,[57] A. A. Alves Jr.,[43] S. Amato,[2] S. Amerio,[24] Y. Amhis,[8] L. An,[18] L. Anderlini,[18] G. Andreassi,[45] M. Andreotti,[17] J. E. Andrews,[62] F. Archilli,[28] P. d'Argent,[13] J. Arnau Romeu,[7] A. Artamonov,[40] M. Artuso,[63] K. Arzymatov,[37] E. Aslanides,[7] M. Atzeni,[46] B. Audurier,[23] S. Bachmann,[13] J. J. Back,[52] S. Baker,[57] V. Balagura,[8,b] W. Baldini,[17] A. Baranov,[37] R. J. Barlow,[58] G. C. Barrand,[8] S. Barsuk,[8] W. Barter,[58] M. Bartolini,[20] F. Baryshnikov,[74] V. Batozskaya,[32] B. Batsukh,[63] A. Battig,[11] V. Battista,[45] A. Bay,[45] J. Beddow,[55] F. Bedeschi,[25] I. Bediaga,[1] A. Beiter,[63] L. J. Bel,[28] S. Belin,[23] N. Beliy,[66] V. Bellee,[45] N. Belloli,[21,I] K. Belous,[40] I. Belyaev,[34] E. Ben-Haim,[9] G. Bencivenni,[19] S. Benson,[28] S. Beranek,[10] A. Berezhnoy,[35] R. Bernet,[46] D. Berninghoff,[13] E. Bertholet,[9] A. Bertolin,[24] C. Betancourt,[46] F. Betti,[16,44] M. O. Bettler,[51] M. van Beuzekom,[28] Ia. Bezshyiko,[46] S. Bhasin,[50] J. Bhom,[30] M. S. Bieker,[11] S. Bifani,[49] P. Billoir,[9] A. Birnkraut,[11] A. Bizzeti,[18,u] M. Bjørn,[59] M. P. Blago,[44] T. Blake,[52] F. Blanc,[45] S. Blusk,[63] D. Bobulska,[55] V. Bocci,[27] O. Boente Garcia,[43] T. Boettcher,[60] A. Bondar,[39,x] N. Bondar,[41] S. Borghi,[58,44] M. Borisyak,[37] M. Borsato,[43] M. Boubdir,[10] T. J. V. Bowcock,[56] C. Bozzi,[17,44] S. Braun,[13] M. Brodski,[44] J. Brodzicka,[30] A. Brossa Gonzalo,[52] D. Brundu,[23,44] E. Buchanan,[50] A. Buonaura,[46] C. Burr,[58] A. Bursche,[23] J. Buytaert,[44] W. Byczynski,[44] S. Cadeddu,[23] H. Cai,[68] R. Calabrese,[17,g] R. Calladine,[49] M. Calvi,[21,i] M. Calvo Gomez,[42,m] A. Camboni,[42,m] P. Campana,[19] D. H. Campora Perez,[44] L. Capriotti,[16,e] A. Carbone,[16,e] G. Carboni,[26] R. Cardinale,[20] A. Cardini,[23] P. Carniti,[21,I] K. Carvalho Akiba,[2] G. Casse,[56] M. Cattaneo,[44] G. Cavallero,[20] R. Cenci,[25,p] D. Chamont,[8] M. G. Chapman,[50] M. Charles,[9] Ph. Charpentier,[44] G. Chatzikonstantinidis,[49] M. Chefdeville,[5] V. Chekalina,[37] C. Chen,[3] S. Chen,[23] S.-G. Chitic,[44] V. Chobanova,[43] M. Chrzaszcz,[44] A. Chubykin,[41] P. Ciambrone,[19] X. Cid Vidal,[43] G. Ciezarek,[44] F. Cindolo,[16] P. E. L. Clarke,[54] M. Clemencic,[44] H. V. Cliff,[51] J. Closier,[44] V. Coco,[44] J. A. B. Coelho,[8] J. Cogan,[7] E. Cogneras,[6] L. Cojocariu,[33] P. Collins,[44] T. Colombo,[44] A. Comerma-Montells,[13] A. Contu,[23] G. Coombs,[44] S. Coquereau,[42] G. Corti,[44] M. Corvo,[17,g] C. M. Costa Sobral,[52] B. Couturier,[44] G. A. Cowan,[54] D. C. Craik,[60] A. Crocombe,[52] M. Cruz Torres,[1] R. Currie,[54] C. D'Ambrosio,[44] F. Da Cunha Marinho,[2] C. L. Da Silva,[78] E. Dall'Occo,[28] J. Dalseno,[43,v] A. Danilina,[34] A. Davis,[58] O. De Aguiar Francisco,[44] K. De Bruyn,[44] S. De Capua,[58] M. De Cian,[45] J. M. De Miranda,[1] L. De Paula,[2] M. De Serio,[15,d] P. De Simone,[19] C. T. Dean,[55] W. Dean,[77] D. Decamp,[5] L. Del Buono,[9] B. Delaney,[51] H.-P. Dembinski,[12] M. Demmer,[11] A. Dendek,[31] D. Derkach,[38] O. Deschamps,[6] F. Desse,[8] F. Dettori,[56]

B. Dey,[69] A. Di Canto,[44] P. Di Nezza,[19] S. Didenko,[74] H. Dijkstra,[44] F. Dordei,[23] M. Dorigo,[44,y] A. Dosil Suárez,[43] L. Douglas,[55] A. Dovbnya,[47] K. Dreimanis,[56] L. Dufour,[44] G. Dujany,[9] P. Durante,[44] J. M. Durham,[78] D. Dutta,[58] R. Dzhelyadin,[40] M. Dziewiecki,[13] A. Dziurda,[30] A. Dzyuba,[41] S. Easo,[53] U. Egede,[57] V. Egorychev,[34] S. Eidelman,[39,x] S. Eisenhardt,[54] U. Eitschberger,[11] R. Ekelhof,[11] L. Eklund,[55] S. Ely,[63] A. Ene,[33] S. Escher,[10] S. Esen,[28] T. Evans,[61] A. Falabella,[16] N. Farley,[49] S. Farry,[56] D. Fazzini,[21,44,I] P. Fernandez Declara,[44] A. Fernandez Prieto,[43] F. Ferrari,[16,e] L. Ferreira Lopes,[45] F. Ferreira Rodrigues,[2] M. Ferro-Luzzi,[44] S. Filippov,[36] R. A. Fini,[15] M. Fiorini,[17,g] M. Firlej,[31] C. Fitzpatrick,[45] T. Fiutowski,[31] F. Fleuret,[8,b] M. Fontana,[44] F. Fontanelli,[20,h] R. Forty,[44] V. Franco Lima,[56] M. Frank,[44] C. Frei,[44] J. Fu,[22,q] W. Funk,[44] C. Färber,[44] M. Féo,[44] E. Gabriel,[54] A. Gallas Torreira,[43] D. Galli,[16,e] S. Gallorini,[24] S. Gambetta,[54] Y. Gan,[3] M. Gandelman,[2] P. Gandini,[22] Y. Gao,[3] L. M. Garcia Martin,[76] B. Garcia Plana,[43] J. García Pardiñas,[46] J. Garra Tico,[51] L. Garrido,[42] D. Gascon,[42] C. Gaspar,[44] L. Gavardi,[11] G. Gazzoni,[6] D. Gerick,[13] E. Gersabeck,[58] M. Gersabeck,[58] T. Gershon,[52] D. Gerstel,[7] Ph. Ghez,[5] V. Gibson,[51] O. G. Girard,[45] P. Gironella Gironell,[42] L. Giubega,[33] K. Gizdov,[54] V. V. Gligorov,[9] D. Golubkov,[34] A. Golutvin,[57,74] A. Gomes,[1,a] I. V. Gorelov,[35] C. Gotti,[21,I] E. Govorkova,[28] J. P. Grabowski,[13] R. Graciani Diaz,[42] L. A. Granado Cardoso,[44] E. Graugés,[42] E. Graverini,[46] G. Graziani,[18] A. Grecu,[33] R. Greim,[28] P. Griffith,[23] L. Grillo,[58] L. Gruber,[44] B. R. Gruberg Cazon,[59] O. Grünberg,[71] C. Gu,[3] E. Gushchin,[36] A. Guth,[10] Yu. Guz,[40,44] T. Gys,[44] C. Göbel,[65] T. Hadavizadeh,[59] C. Hadjivasiliou,[6] G. Haefeli,[45] C. Haen,[44] S. C. Haines,[51] B. Hamilton,[62] X. Han,[13] T. H. Hancock,[59] S. Hansmann-Menzemer,[13] N. Harnew,[59] T. Harrison,[56] C. Hasse,[44] M. Hatch,[44] J. He,[66] M. Hecker,[57] K. Heinicke,[11] A. Heister,[11] K. Hennessy,[56] L. Henry,[76] E. van Herwijnen,[44] J. Heuel,[10] M. Heß,[71] A. Hicheur,[64] R. Hidalgo Charman,[58] D. Hill,[59] M. Hilton,[58] P. H. Hopchev,[45] J. Hu,[13] W. Hu,[69] W. Huang,[66] Z. C. Huard,[61] W. Hulsbergen,[28] T. Humair,[57] M. Hushchyn,[38] D. Hutchcroft,[56] D. Hynds,[28] P. Ibis,[11] M. Idzik,[31] P. Ilten,[49] A. Inglessi,[41] A. Inyakin,[40] K. Ivshin,[41] R. Jacobsson,[44] J. Jalocha,[59] E. Jans,[28] B. K. Jashal,[76] A. Jawahery,[62] F. Jiang,[3] M. John,[59] D. Johnson,[44] C. R. Jones,[51] C. Joram,[44] B. Jost,[44] N. Jurik,[59] S. Kandybei,[47] M. Karacson,[44] J. M. Kariuki,[50] S. Karodia,[55] N. Kazeev,[38] M. Kecke,[13] F. Keizer,[51] M. Kelsey,[63] M. Kenzie,[51] T. Ketel,[29] E. Khairullin,[37] B. Khanji,[44] C. Khurewathanakul,[45] K. E. Kim,[63] T. Kirn,[10] V. S. Kirsebom,[45] S. Klaver,[19] K. Klimaszewski,[32] T. Klimkovich,[12] S. Koliiev,[48] M. Kolpin,[13] R. Kopecna,[13] P. Koppenburg,[28] I. Kostiuk,[28,48] S. Kotriakhova,[41] M. Kozeiha,[6] L. Kravchuk,[36] M. Kreps,[52] F. Kress,[57] P. Krokovny,[39,x] W. Krupa,[31] W. Krzemien,[32] W. Kucewicz,[30,l] M. Kucharczyk,[30] V. Kudryavtsev,[39,x] A. K. Kuonen,[45] T. Kvaratskheliya,[34,44] D. Lacarrere,[44] G. Lafferty,[58] A. Lai,[23] D. Lancierini,[46] G. Lanfranchi,[19] C. Langenbruch,[10] T. Latham,[52] C. Lazzeroni,[49] R. Le Gac,[7] A. Leflat,[35] R. Lefèvre,[6] F. Lemaitre,[44] O. Leroy,[7] T. Lesiak,[30] B. Leverington,[13] P.-R. Li,[66,ab] Y. Li,[4] Z. Li,[63] X. Liang,[63] T. Likhomanenko,[73] R. Lindner,[44] F. Lionetto,[46] V. Lisovskyi,[8] G. Liu,[67] X. Liu,[3] D. Loh,[52] A. Loi,[23] I. Longstaff,[55] J. H. Lopes,[2] G. H. Lovell,[51] D. Lucchesi,[24,o] M. Lucio Martinez,[43] Y. Luo,[3] A. Lupato,[24] E. Luppi,[17,g] O. Lupton,[44] A. Lusiani,[25] X. Lyu,[66] F. Machefert,[8] F. Maciuc,[33] V. Macko,[45] P. Mackowiak,[11] S. Maddrell-Mander,[50] O. Maev,[41,44] K. Maguire,[58] D. Maisuzenko,[41] M. W. Majewski,[31] S. Malde,[59] B. Malecki,[44] A. Malinin,[73] T. Maltsev,[39,x] H. Malygina,[13] G. Manca,[23,f] G. Mancinelli,[7] D. Marangotto,[22,q] J. Maratas,[6,w] J. F. Marchand,[5] U. Marconi,[16] C. Marin Benito,[8] M. Marinangeli,[45] P. Marino,[45] J. Marks,[13] P. J. Marshall,[56] G. Martellotti,[27] M. Martinelli,[44] D. Martinez Santos,[43] F. Martinez Vidal,[76] A. Massafferri,[1] M. Materok,[10] R. Matev,[44] A. Mathad,[52] Z. Mathe,[44] C. Matteuzzi,[21] A. Mauri,[46] E. Maurice,[8,b] B. Maurin,[45] M. McCann,[57,44] A. McNab,[58] R. McNulty,[14] J. V. Mead,[56] B. Meadows,[61] C. Meaux,[7] N. Meinert,[71] D. Melnychuk,[32] M. Merk,[28] A. Merli,[22,q] E. Michielin,[24] D. A. Milanes,[70] E. Millard,[52] M.-N. Minard,[5] L. Minzoni,[17,g] D. S. Mitzel,[13] A. Mogini,[9] R. D. Moise,[57] T. Mombächer,[11] I. A. Monroy,[70] S. Monteil,[6] M. Morandin,[24] G. Morello,[19] M. J. Morello,[25,t] O. Morgunova,[73] J. Moron,[31] A. B. Morris,[7] R. Mountain,[63] F. Muheim,[54] M. Mukherjee,[69] M. Mulder,[28] C. H. Murphy,[59] D. Murray,[58] A. Mödden,[11] D. Müller,[44] J. Müller,[11] K. Müller,[46] V. Müller,[11] P. Naik,[50] T. Nakada,[45] R. Nandakumar,[53] A. Nandi,[59] T. Nanut,[45] I. Nasteva,[2] M. Needham,[54] N. Neri,[22,q] S. Neubert,[13] N. Neufeld,[44] R. Newcombe,[57] T. D. Nguyen,[45] C. Nguyen-Mau,[45,n] S. Nieswand,[10] R. Niet,[11] N. Nikitin,[35] A. Nogay,[73] N. S. Nolte,[44] D. P. O'Hanlon,[16] A. Oblakowska-Mucha,[31] V. Obraztsov,[40] S. Ogilvy,[55] R. Oldeman,[23,f] C. J. G. Onderwater,[72] A. Ossowska,[30] J. M. Otalora Goicochea,[2] T. Ovsiannikova,[34] P. Owen,[46] A. Oyanguren,[76] P. R. Pais,[45] T. Pajero,[25,t] A. Palano,[15] M. Palutan,[19] G. Panshin,[75] A. Papanestis,[53] M. Pappagallo,[54] L. L. Pappalardo,[17,g] W. Parker,[62] C. Parkes,[58,44] G. Passaleva,[18,44] A. Pastore,[15] M. Patel,[57] C. Patrignani,[16,e] A. Pearce,[44] A. Pellegrino,[28] G. Penso,[27] M. Pepe Altarelli,[44] S. Perazzini,[44] D. Pereima,[34] P. Perret,[6] L. Pescatore,[45] K. Petridis,[50] A. Petrolini,[20,h] A. Petrov,[73] S. Petrucci,[54] M. Petruzzo,[22,q] B. Pietrzyk,[5] G. Pietrzyk,[45] M. Pikies,[30] M. Pili,[59] D. Pinci,[27] J. Pinzino,[44] F. Pisani,[44] A. Piucci,[13] V. Placinta,[33] S. Playfer,[54] J. Plews,[49] M. Plo Casasus,[43] F. Polci,[9] M. Poli Lener,[19] A. Poluektov,[7] N. Polukhina,[74,c]

I. Polyakov,[63] E. Polycarpo,[2] G. J. Pomery,[50] S. Ponce,[44] A. Popov,[40] D. Popov,[49,12] S. Poslavskii,[40] E. Price,[50] J. Prisciandaro,[43] C. Prouve,[43] V. Pugatch,[48] A. Puig Navarro,[46] H. Pullen,[59] G. Punzi,[25,p] W. Qian,[66] J. Qin,[66] R. Quagliani,[9] B. Quintana,[6] N. V. Raab,[14] B. Rachwal,[31] J. H. Rademacker,[50] M. Rama,[25] M. Ramos Pernas,[43] M. S. Rangel,[2] F. Ratnikov,[37,38] G. Raven,[29] M. Ravonel Salzgeber,[44] M. Reboud,[5] F. Redi,[45] S. Reichert,[11] A. C. dos Reis,[1] F. Reiss,[9] C. Remon Alepuz,[76] Z. Ren,[3] V. Renaudin,[59] S. Ricciardi,[53] S. Richards,[50] K. Rinnert,[56] P. Robbe,[8] A. Robert,[9] A. B. Rodrigues,[45] E. Rodrigues,[61] J. A. Rodriguez Lopez,[70] M. Roehrken,[44] S. Roiser,[44] A. Rollings,[59] V. Romanovskiy,[40] A. Romero Vidal,[43] J. D. Roth,[77] M. Rotondo,[19] M. S. Rudolph,[63] T. Ruf,[44] J. Ruiz Vidal,[76] J. J. Saborido Silva,[43] N. Sagidova,[41] B. Saitta,[23,f] V. Salustino Guimaraes,[65] C. Sanchez Gras,[28] C. Sanchez Mayordomo,[76] B. Sanmartin Sedes,[43] R. Santacesaria,[27] C. Santamarina Rios,[43] M. Santimaria,[19,44] E. Santovetti,[26,j] G. Sarpis,[58] A. Sarti,[19,k] C. Satriano,[27,s] A. Satta,[26] M. Saur,[66] D. Savrina,[34,35] S. Schael,[10] M. Schellenberg,[11] M. Schiller,[55] H. Schindler,[44] M. Schmelling,[12] T. Schmelzer,[11] B. Schmidt,[44] O. Schneider,[45] A. Schopper,[44] H. F. Schreiner,[61] M. Schubiger,[45] S. Schulte,[45] M. H. Schune,[8] R. Schwemmer,[44] B. Sciascia,[19] A. Sciubba,[27,k] A. Semennikov,[34] E. S. Sepulveda,[9] A. Sergi,[49] N. Serra,[46] J. Serrano,[7] L. Sestini,[24] A. Seuthe,[11] P. Seyfert,[44] M. Shapkin,[40] Y. Shcheglov,[41] T. Shears,[56] L. Shekhtman,[39,x] V. Shevchenko,[73] E. Shmanin,[74] B. G. Siddi,[17] R. Silva Coutinho,[46] L. Silva de Oliveira,[2] G. Simi,[24,o] S. Simone,[15,d] I. Skiba,[17] N. Skidmore,[13] T. Skwarnicki,[63] M. W. Slater,[49] J. G. Smeaton,[51] E. Smith,[10] I. T. Smith,[54] M. Smith,[57] M. Soares,[16] l. Soares Lavra,[1] M. D. Sokoloff,[61] F. J. P. Soler,[55] B. Souza De Paula,[2] B. Spaan,[11] E. Spadaro Norella,[22,q] P. Spradlin,[55] F. Stagni,[44] M. Stahl,[13] S. Stahl,[44] P. Stefko,[45] S. Stefkova,[57] O. Steinkamp,[46] S. Stemmle,[13] O. Stenyakin,[40] M. Stepanova,[41] H. Stevens,[11] A. Stocchi,[8] S. Stone,[63] B. Storaci,[46] S. Stracka,[25] M. E. Stramaglia,[45] M. Straticiuc,[33] U. Straumann,[46] S. Strokov,[75] J. Sun,[3] L. Sun,[68] Y. Sun,[62] K. Swientek,[31] A. Szabelski,[32] T. Szumlak,[31] M. Szymanski,[66] S. T'Jampens,[5] Z. Tang,[3] T. Tekampe,[11] G. Tellarini,[17] F. Teubert,[44] E. Thomas,[44] J. van Tilburg,[28] M. J. Tilley,[57] V. Tisserand,[6] M. Tobin,[31] S. Tolk,[44] L. Tomassetti,[17,g] D. Tonelli,[25] D. Y. Tou,[9] R. Tourinho Jadallah Aoude,[1] E. Tournefier,[5] M. Traill,[55] M. T. Tran,[45] A. Trisovic,[51] A. Tsaregorodtsev,[7] G. Tuci,[25,p] A. Tully,[51] N. Tuning,[28,44] A. Ukleja,[32] A. Usachov,[8] A. Ustyuzhanin,[37,38] U. Uwer,[13] A. Vagner,[75] V. Vagnoni,[16] A. Valassi,[44] S. Valat,[44] G. Valenti,[16] R. Vazquez Gomez,[44] P. Vazquez Regueiro,[43] S. Vecchi,[17] M. van Veghel,[28] J. J. Velthuis,[50] M. Veltri,[18,r] G. Veneziano,[59] A. Venkateswaran,[63] M. Vernet,[6] M. Veronesi,[28] M. Vesterinen,[52] J. V. Viana Barbosa,[44] D. Vieira,[66] M. Vieites Diaz,[43] H. Viemann,[71] X. Vilasis-Cardona,[42,m] A. Vitkovskiy,[28] M. Vitti,[51] V. Volkov,[35] A. Vollhardt,[46] D. Vom Bruch,[9] B. Voneki,[44] A. Vorobyev,[41] V. Vorobyev,[39,x] N. Voropaev,[41] J. A. de Vries,[28] C. Vázquez Sierra,[28] R. Waldi,[71] J. Walsh,[25] J. Wang,[4] M. Wang,[3] Y. Wang,[69] Z. Wang,[46] D. R. Ward,[51] H. M. Wark,[56] N. K. Watson,[49] D. Websdale,[57] A. Weiden,[46] C. Weisser,[60] M. Whitehead,[10] G. Wilkinson,[59] M. Wilkinson,[63] I. Williams,[51] M. R. J. Williams,[58] M. Williams,[60] T. Williams,[49] F. F. Wilson,[53] M. Winn,[8] W. Wislicki,[32] M. Witek,[30] G. Wormser,[8] S. A. Wotton,[51] K. Wyllie,[44] D. Xiao,[69] Y. Xie,[69] A. Xu,[3] M. Xu,[69] Q. Xu,[66] Z. Xu,[3] Z. Xu,[5] Z. Yang,[3] Z. Yang,[62] Y. Yao,[63] L. E. Yeomans,[56] H. Yin,[69] J. Yu,[69,aa] X. Yuan,[63] O. Yushchenko,[40] K. A. Zarebski,[49] M. Zavertyaev,[12,c] D. Zhang,[69] L. Zhang,[3] W. C. Zhang,[3,z] Y. Zhang,[44] A. Zhelezov,[13] Y. Zheng,[66] X. Zhu,[3] V. Zhukov,[10,35] J. B. Zonneveld,[54] and S. Zucchelli[16,e]

(LHCb Collaboration)

[1]*Centro Brasileiro de Pesquisas Físicas (CBPF), Rio de Janeiro, Brazil*
[2]*Universidade Federal do Rio de Janeiro (UFRJ), Rio de Janeiro, Brazil*
[3]*Center for High Energy Physics, Tsinghua University, Beijing, China*
[4]*Institute Of High Energy Physics (ihep), Beijing, China*
[5]*University Grenoble Alpes, University Savoie Mont Blanc, CNRS, IN2P3-LAPP, Annecy, France*
[6]*Université Clermont Auvergne, CNRS/IN2P3, LPC, Clermont-Ferrand, France*
[7]*Aix Marseille Univ, CNRS/IN2P3, CPPM, Marseille, France*
[8]*LAL, University Paris-Sud, CNRS/IN2P3, Université Paris-Saclay, Orsay, France*
[9]*LPNHE, Sorbonne Université, Paris Diderot Sorbonne Paris Cité, CNRS/IN2P3, Paris, France*
[10]*I. Physikalisches Institut, RWTH Aachen University, Aachen, Germany*
[11]*Fakultät Physik, Technische Universität Dortmund, Dortmund, Germany*
[12]*Max-Planck-Institut für Kernphysik (MPIK), Heidelberg, Germany*
[13]*Physikalisches Institut, Ruprecht-Karls-Universität Heidelberg, Heidelberg, Germany*
[14]*School of Physics, University College Dublin, Dublin, Ireland*
[15]*INFN Sezione di Bari, Bari, Italy*
[16]*INFN Sezione di Bologna, Bologna, Italy*

[17]*INFN Sezione di Ferrara, Ferrara, Italy*
[18]*INFN Sezione di Firenze, Firenze, Italy*
[19]*INFN Laboratori Nazionali di Frascati, Frascati, Italy*
[20]*INFN Sezione di Genova, Genova, Italy*
[21]*INFN Sezione di Milano-Bicocca, Milano, Italy*
[22]*INFN Sezione di Milano, Milano, Italy*
[23]*INFN Sezione di Cagliari, Monserrato, Italy*
[24]*INFN Sezione di Padova, Padova, Italy*
[25]*INFN Sezione di Pisa, Pisa, Italy*
[26]*INFN Sezione di Roma Tor Vergata, Roma, Italy*
[27]*INFN Sezione di Roma La Sapienza, Roma, Italy*
[28]*Nikhef National Institute for Subatomic Physics, Amsterdam, Netherlands*
[29]*Nikhef National Institute for Subatomic Physics and VU University Amsterdam, Amsterdam, Netherlands*
[30]*Henryk Niewodniczanski Institute of Nuclear Physics Polish Academy of Sciences, Kraków, Poland*
[31]*AGH - University of Science and Technology, Faculty of Physics and Applied Computer Science, Kraków, Poland*
[32]*National Center for Nuclear Research (NCBJ), Warsaw, Poland*
[33]*Horia Hulubei National Institute of Physics and Nuclear Engineering, Bucharest-Magurele, Romania*
[34]*Institute of Theoretical and Experimental Physics (ITEP), Moscow, Russia*
[35]*Institute of Nuclear Physics, Moscow State University (SINP MSU), Moscow, Russia*
[36]*Institute for Nuclear Research of the Russian Academy of Sciences (INR RAS), Moscow, Russia*
[37]*Yandex School of Data Analysis, Moscow, Russia*
[38]*National Research University Higher School of Economics, Moscow, Russia*
[39]*Budker Institute of Nuclear Physics (SB RAS), Novosibirsk, Russia*
[40]*Institute for High Energy Physics (IHEP), Protvino, Russia*
[41]*Konstantinov Nuclear Physics Institute of National Research Centre "Kurchatov Institute", PNPI, St.Petersburg, Russia*
[42]*ICCUB, Universitat de Barcelona, Barcelona, Spain*
[43]*Instituto Galego de Física de Altas Enerxías (IGFAE), Universidade de Santiago de Compostela, Santiago de Compostela, Spain*
[44]*European Organization for Nuclear Research (CERN), Geneva, Switzerland*
[45]*Institute of Physics, Ecole Polytechnique Fédérale de Lausanne (EPFL), Lausanne, Switzerland*
[46]*Physik-Institut, Universität Zürich, Zürich, Switzerland*
[47]*NSC Kharkiv Institute of Physics and Technology (NSC KIPT), Kharkiv, Ukraine*
[48]*Institute for Nuclear Research of the National Academy of Sciences (KINR), Kyiv, Ukraine*
[49]*University of Birmingham, Birmingham, United Kingdom*
[50]*H.H. Wills Physics Laboratory, University of Bristol, Bristol, United Kingdom*
[51]*Cavendish Laboratory, University of Cambridge, Cambridge, United Kingdom*
[52]*Department of Physics, University of Warwick, Coventry, United Kingdom*
[53]*STFC Rutherford Appleton Laboratory, Didcot, United Kingdom*
[54]*School of Physics and Astronomy, University of Edinburgh, Edinburgh, United Kingdom*
[55]*School of Physics and Astronomy, University of Glasgow, Glasgow, United Kingdom*
[56]*Oliver Lodge Laboratory, University of Liverpool, Liverpool, United Kingdom*
[57]*Imperial College London, London, United Kingdom*
[58]*School of Physics and Astronomy, University of Manchester, Manchester, United Kingdom*
[59]*Department of Physics, University of Oxford, Oxford, United Kingdom*
[60]*Massachusetts Institute of Technology, Cambridge, Massachusetts, USA*
[61]*University of Cincinnati, Cincinnati, Ohio, USA*
[62]*University of Maryland, College Park, Maryland, USA*
[63]*Syracuse University, Syracuse, New York, USA*
[64]*Laboratory of Mathematical and Subatomic Physics, Constantine, Algeria (associated with Institution Universidade Federal do Rio de Janeiro (UFRJ), Rio de Janeiro, Brazil)*
[65]*Pontifícia Universidade Católica do Rio de Janeiro (PUC-Rio), Rio de Janeiro, Brazil [associated with Institution Universidade Federal do Rio de Janeiro (UFRJ), Rio de Janeiro, Brazil]*
[66]*University of Chinese Academy of Sciences, Beijing, China (associated with Institution Center for High Energy Physics, Tsinghua University, Beijing, China)*
[67]*South China Normal University, Guangzhou, China (associated with Institution Center for High Energy Physics, Tsinghua University, Beijing, China)*
[68]*School of Physics and Technology, Wuhan University, Wuhan, China (associated with Institution Center for High Energy Physics, Tsinghua University, Beijing, China)*

[69]*Institute of Particle Physics, Central China Normal University, Wuhan, Hubei, China*
(associated with Institution Center for High Energy Physics, Tsinghua University, Beijing, China)
[70]*Departamento de Fisica, Universidad Nacional de Colombia, Bogota, Colombia*
(associated with Institution LPNHE, Sorbonne Université, Paris Diderot Sorbonne Paris Cité, CNRS/IN2P3, Paris, France)
[71]*Institut für Physik, Universität Rostock, Rostock, Germany*
(associated with Institution Physikalisches Institut, Ruprecht-Karls-Universität Heidelberg, Heidelberg, Germany)
[72]*Van Swinderen Institute, University of Groningen, Groningen, Netherlands*
(associated with Institution Nikhef National Institute for Subatomic Physics, Amsterdam, Netherlands)
[73]*National Research Centre Kurchatov Institute, Moscow, Russia*
(associated with Institution Institute of Theoretical and Experimental Physics (ITEP), Moscow, Russia)
[74]*National University of Science and Technology "MISIS", Moscow, Russia*
(associated with Institution Institute of Theoretical and Experimental Physics (ITEP), Moscow, Russia)
[75]*National Research Tomsk Polytechnic University, Tomsk, Russia*
(associated with Institution Institute of Theoretical and Experimental Physics (ITEP), Moscow, Russia)
[76]*Instituto de Fisica Corpuscular, Centro Mixto Universidad de Valencia - CSIC, Valencia, Spain*
(associated with Institution ICCUB, Universitat de Barcelona, Barcelona, Spain)
[77]*University of Michigan, Ann Arbor, United States*
(associated with Institution Syracuse University, Syracuse, NY, United States)
[78]*Los Alamos National Laboratory (LANL), Los Alamos, United States*
(associated with Institution Syracuse University, Syracuse, NY, United States)

[a]Also at Universidade Federal do Triângulo Mineiro (UFTM), Uberaba-MG, Brazil.
[b]Also at Laboratoire Leprince-Ringuet, Palaiseau, France.
[c]Also at P.N. Lebedev Physical Institute, Russian Academy of Science (LPI RAS), Moscow, Russia.
[d]Also at Università di Bari, Bari, Italy.
[e]Also at Università di Bologna, Bologna, Italy.
[f]Also at Università di Cagliari, Cagliari, Italy.
[g]Also at Università di Ferrara, Ferrara, Italy.
[h]Also at Università di Genova, Genova, Italy.
[i]Also at Università di Milano Bicocca, Milano, Italy.
[j]Also at Università di Roma Tor Vergata, Roma, Italy.
[k]Also at Università di Roma La Sapienza, Roma, Italy.
[l]Also at AGH - University of Science and Technology, Faculty of Computer Science, Electronics and Telecommunications, Kraków, Poland.
[m]Also at LIFAELS, La Salle, Universitat Ramon Llull, Barcelona, Spain.
[n]Also at Hanoi University of Science, Hanoi, Vietnam.
[o]Also at Università di Padova, Padova, Italy.
[p]Also at Università di Pisa, Pisa, Italy.
[q]Also at Università degli Studi di Milano, Milano, Italy.
[r]Also at Università di Urbino, Urbino, Italy.
[s]Also at Università della Basilicata, Potenza, Italy.
[t]Also at Scuola Normale Superiore, Pisa, Italy.
[u]Also at Università di Modena e Reggio Emilia, Modena, Italy.
[v]Also at H.H. Wills Physics Laboratory, University of Bristol, Bristol, United Kingdom.
[w]Also at MSU - Iligan Institute of Technology (MSU-IIT), Iligan, Philippines.
[x]Also at Novosibirsk State University, Novosibirsk, Russia.
[y]Also at Sezione INFN di Trieste, Trieste, Italy.
[z]Also at School of Physics and Information Technology, Shaanxi Normal University (SNNU), Xi'an, China.
[aa]Also at Physics and Micro Electronic College, Hunan University, Changsha City, China.
[ab]Also at Lanzhou University, Lanzhou, China.